A LOW PRESSURE AXIAL FAN FOR BENCHMARKING PREDICTION METHODS FOR AERODYNAMIC PERFORMANCE AND SOUND

Thomas CAROLUS, Tao ZHU, Michael STURM

University of Siegen, Institute for Fluid- and Thermodynamics
Paul-Bonatz-Strasse 9-11, D-57068 Siegen, Germany

SUMMARY

Great efforts into implementing numerical methods for performance and sound prediction can be observed in the fan and blower industry. Trust in results from simulation, however, often relies on experimental validation. The purpose of this paper is to describe the low pressure rotor-only fan "USI7" which has been used as a generic test fan in several projects at the University of Siegen and elsewhere for several years. We present our own experimental results such as performance and sound characteristics, turbulent inflow statistics and sound spectra as well as the test rigs employed to obtain the data. The idea behind is to foster benchmarking of present and new steady-state and unsteady aerodynamic and aero-acoustic prediction methods within the community. Thus, to any individual we will provide full geometry of the fan as well as all experimental data.

INTRODUCTION

Utilization of numerical methods for performance and sound prediction is well established in the turbo machinery community. Numerous flow simulation and sound field prediction codes are on the market, many more under development and test in research establishments. E.g. Reynolds-averaged Navier-Stokes (RANS) codes are regarded as a mature tool, and unsteady methods such as large eddy simulation (LES) and the Lattice-Boltzmann method (LBM) gain ground because of the demand from aero-acousticians and structural health engineers. Not only designers of complex machines such as aircraft engines try to take advantage of simulation methods. Great efforts into implementing those methods in its design process can also be observed in the mass-producing fan and blower industry. Typically CFD yields a huge amount of detailed flow field data which then need to be processed further to obtain overall machine characteristics such as pressure rise, efficiency, level of emitted sound power etc. Hence, at every stage of the simulation validation by experiments is a serious issue. But the generation of sound experimental data is often very costly, and often the boundary conditions for specific experiments are documented inadequately. The objective of this

paper is to describe a low pressure fan which was used as a generic test fan in several projects during the last years at the University of Siegen [1 - 6] and elsewhere and to present our own experimental results such as performance and sound characteristics, turbulent inflow statistics and far field sound spectra. A further objective is to present the test rigs which were used to obtain those data.

DESIGN PHILOSOPHY AND FAN GEOMETRY

The University of Siegen axial fan "USI7" is a low pressure rotor-only fan with a low solidity blade cascade, Fig. 1. Its operational range in terms of volume flow rate and pressure rise is more or less typical for a large class of assembly-line produced fans. The lack of outlet guide vanes stems from the fact that the potential pressure recovery due to guide vanes is comparably small. A design without guide vanes, however, implies that the dynamic pressure at the fan's outlet not only contains kinetic energy associated with the axial but the circumferential flow velocity as well.

The blade design is based on blade element theory combined with XFOIL-predicted airfoil lift and drag data. For that the public domain code XFOIL for analysis of subsonic isolated airfoils by Drela [7] has been integrated in the existing in-house fan design code "dAX" [8]. The blades are loaded only moderately. The objective was to reduce secondary flow phenomena in the blade passages and local flow separation as much as possible. Each fan blade is set up by 15 classical 4-digit NACA airfoil sections with a relative thickness varying from 8 % at the hub to 7 % at the tip. Blade skew is introduced mainly because of noise reasons and taken into account by a spanwise chord length correction. The nominal diameter of the rotor is 300 mm. The chord length of each blade varies from some 86 mm at the hub to 68 mm at the tip. The thickness of the blade trailing edge is 0.6 mm. The design rotational speed is 3000 rpm. Note that the chosen diameter and rotational speed lead to relatively low values of Reynolds and circumferential Mach number, which, nevertheless, are typical for similar assembly-line produced fans. Tab. 1 summarizes the important design parameters.

Table 1: Design parameters of the fan USI7

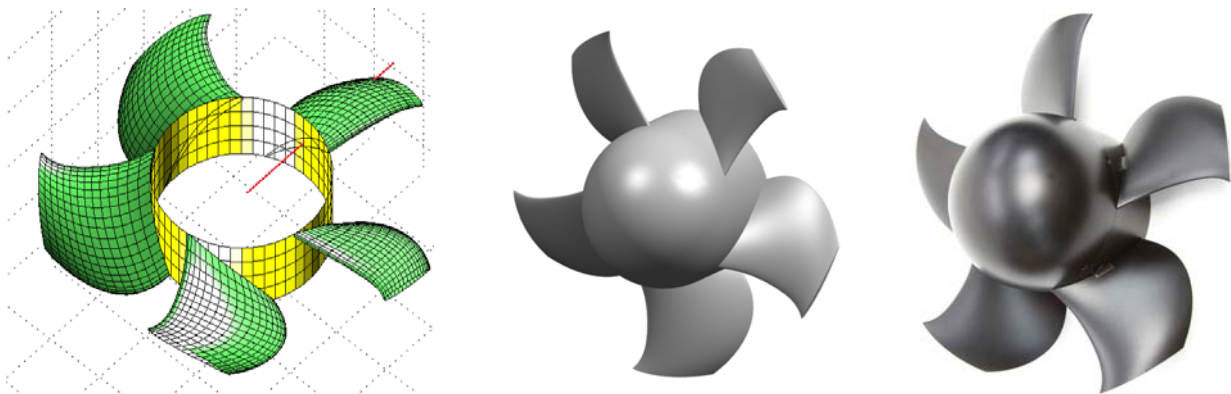|		
Nominal rotor diameter	d_2	300 mm
Hub diameter	d_1	135 mm
Rotational speed	n	3000 rpm
Design flow rate	$\dot{V}_{design}$	0.65 m^3/s
Number of blades	z	5
Circumferential Mach number at d_2	$Ma = \pi d_2 n / a$	0.139
Reynolds number at d_2	$Re = Cw_\infty / \nu$	2.1·10^5

Figure 1: Rotor USI7; left: Design with blade element momentum theory - 15 blade elements along span; middle: 3D-CAD model; right: Manufactured from aluminium by 3D CNC-milling (blades mounted on cylindrical hub)

Fig. 2 shows the fan assembly. The rotor "USI7" is placed in a precision aluminium tube with a clear diameter of 300 mm. The rotor's nominal diameter is reduced slightly in order to provide the desired tip gap by precision milling. The experimental results reported below had been obtained with two different tip gaps, i.e. the clearance between blade tip and housing: 0.3 and 3.0 mm which correspond to 0.1 % and 1 % of nominal rotor diameter d_2, respectively. The spinner is a hemisphere attached smoothly to the cylindrical hub (diameter 135 mm). Two sets of three thin cylindrical struts (threaded rods M8) hold the complete rotor unit in the tube. The first set is placed 300 mm downstream of the rotor (i.e. one rotor diameter), the second another 370 mm. That position of the struts is thought to avoid rotor/stator interaction and its resulting in tonal sound.
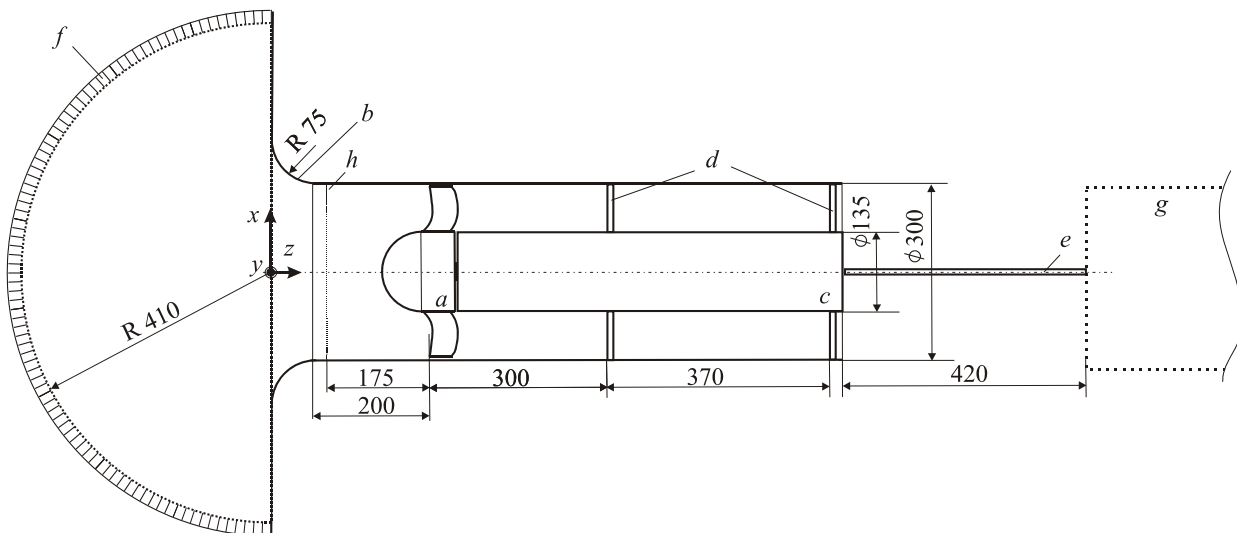

Figure 2: Fan assembly; (a) impeller "USI 7" with hemispherical spinner, (b) bell mouth inlet nozzle, (c) bearing and electric drive, (d) two sets of three cylindrical struts (threaded rods M8, equally spaced on circumference), (e) optional external drive shaft (see Fig. 3), (f) hemispherical flow conditioner (HFC), (g) blocked volume by optional external electric motor with integrated torque shaft (see Fig. 3), (h) measuring plane for hot wire inflow measurements

A hemispherical flow conditioner (HFC), in essence a turbulence control device, is flange mounted to the bell mouth nozzle. It serves to homogenize the potentially disturbed inflow and to ensure a well defined turbulence (turbulent intensity as well as correlation length) to the rotor. The HFC is made of a 30 mm thick layer of a flexible honeycomb structure and a wire mesh [9 - 11]. Experiments proved that its pressure loss, acoustic damping and self noise are negligible.

Two variants of the drive are used: Either an external electric motor with an integrated high precision torque shaft or an internal low noise electric motor hidden in the long hub. The first one is used when determining the aerodynamic fan characteristics (pressure rise and efficiency vs. volume flow rate), the second mainly for acoustic and inflow turbulence measurements.

TEST RIGS AT THE UNIVERSITY OF SIEGEN

Two different test rigs are employed for all measurements reported here. Fig. 3 shows the chamber test rig for aerodynamic performance testing according to the German standard DIN 24163 [12]. The diameter of the cylindrical test rig chamber is large as compared with the rotor diameter, hence in very good approximation the total-to-static pressure rise Δp_{ts} is the pressure differential of the ambient atmosphere to the chamber pressure Δp_{ch}. The volume flow rate is determined from Δp_{nozzle} at the calibrated flow rate metering nozzle. The electric motor in the hub is not active (actually it is removed) and the external electric motor with its integrated torque shaft is used as the fan drive. Prior to all fan measurements the frictional torque due to all bearings between torque shaft and fan

rotor is determined with the fan rotor being removed. Being M the true rotor torque the total-to-static efficiency it obtained as

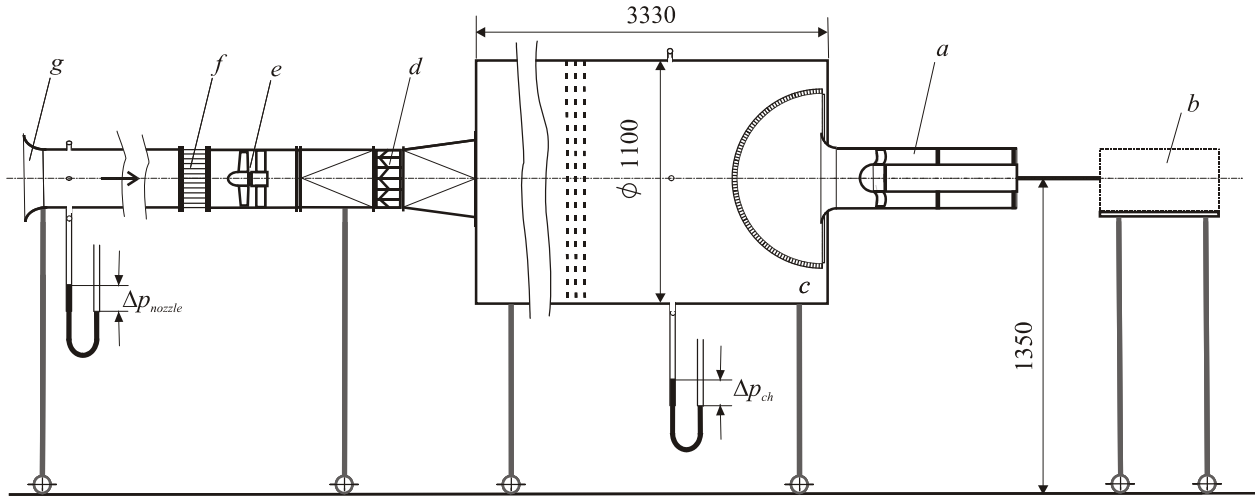$$\eta_{ts} = \frac{\dot{V} \Delta p_{ts}}{2\pi n M}.$$

(1)

Figure 3: Chamber test rig; (a) fan assembly; (b) electric motor with integrated torque meter, (c) settling chamber with internal screens, (d) adjustable throttle, (e) auxiliary fan, (f) flow straightener, (g) volume flow rate metering nozzle

Acoustic measurements are conducted on a duct test rig for fans according to DIN ISO 5136 [13], Fig. 4. The impeller takes the air from a large plenum, designed as a semi-anechoic chamber (i.e. absorbing walls and reflecting ground) and exhausts into a duct with an anechoic termination. The downstream sound power level L_{w4} in the exhausting duct is

$$L_{W4}(f) = L_{p4}(f) + 10\log\frac{A_K}{A_0} + 10\log\frac{(\rho c)_0}{\rho c} + C_{\Sigma}(f).$$

(2)

L_{p4} is measured in the duct by a single microphone mounted four meter downstream of the impeller with a slit tube and a nose cone to cancel out pseudo sound and avoid duct mode effects. A_K is the cross-sectional area of the duct and C_{Σ} the corrections according to [13].

The upstream inlet side sound pressure level L_{p5} is measured in the free field of the semi-anechoic chamber. In a pre-study 16 microphones were placed on a parallelepiped enclosing the bellmouth fan inlet nozzle and the reflecting ground according to ISO 13347-3 [14]. This costly method eventually was replaced by a set of three microphones, placed on a hemispherical arc around the inlet in a distance of $r = 1.3$ m from the fan's spinner and 1350 mm above ground. Then the measurement surface area was taken as $A_M = 2\pi r^2$ and the sound power obtained by

$$L_{W5}(f) = 10\log(\frac{1}{3}\sum_{i=1}^{3}10^{0,1 \cdot L_{p5,i}(f)}) + 10\log\frac{A_M}{A_0} + 10\log\frac{(\rho a)_0}{\rho a}$$

(3)

with the reference area $A_0 = 1$ m^2 and the characteristic acoustic impedance $(\rho a)_0 = 400$ kg/m^{2}s. It was proven that the overall and spectral sound power levels obtained from the 16 and three microphones agreed well within the ensured uncertainty [15].

The fan's volume flow rate is controlled by an adjustable throttle downstream of the termination and is determined by a calibrated hot film probe in the duct. No auxiliary fan is incorporated in order to avoid any acoustic contamination.
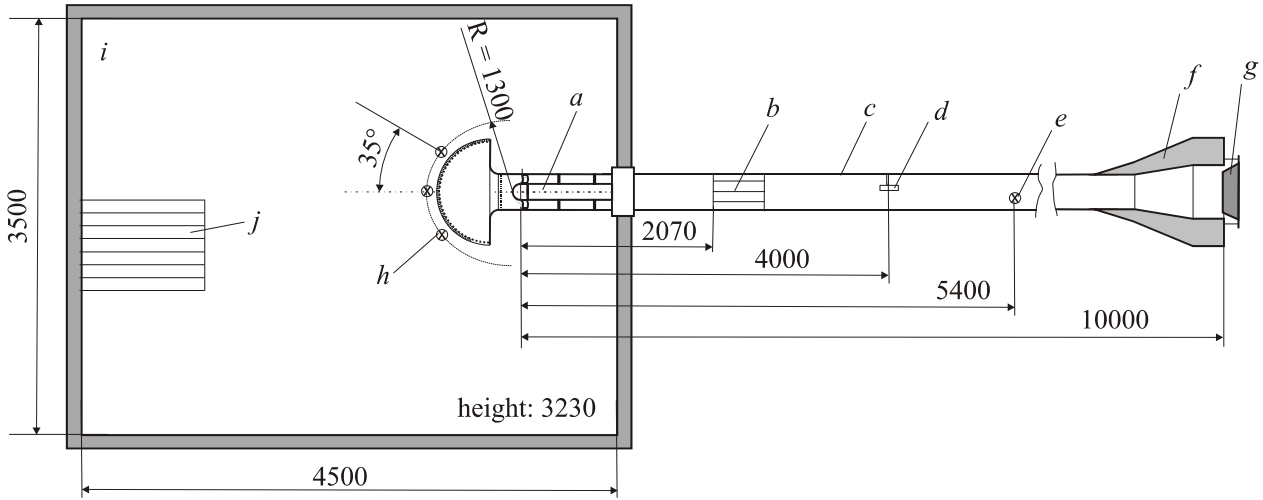
Figure 4: Duct test rig with semi-anechoic chamber (top view); (a) fan assembly with turbulence control screen (center line 1350 mm above reflecting ground), (b) star flow straightener, (c) duct, (d) induct microphone, (e) hot film mass flow meter, (f) anechoic termination, (g) adjustable throttle, (h) free field microphones, (i) semi-anechoic chamber, (j) air inlet grid in reflecting ground

This duct test rig with the fan assembly and the hemispherical flow conditioner attached is also used for determining the turbulent inflow statistics in a measuring plane *h* as marked in Fig. 2. The reference plane is located in a distance 175 mm upstream of the rotor. A 1D hot-wire probe (TSI type 1210-T1.5 in support type 1155) on the anemometer system Dantec Streamline 90N10 is used. The anemometer operates in constant-temperature mode. The measured signals are temperature corrected by utilizing a temperature probe (A8B from Dantec Dynamics). A 24-bit data acquisition system (Module PXI-4495 from National Instruments) is used. The probe is calibrated in a low turbulence wind tunnel. All measurements are conducted over a time interval of one second with a sampling rate of $f_s = 25.6$ kHz. For the spectral analysis standard MATLAB routines (Version 7.0.4, R14) of the The Mathworks Inc. are employed. The power spectral density of the inflow velocity fluctuations

$$E_x\left(f\right)=\frac{d\overline{c_z'^2}}{df} \tag{4}$$

is obtained with the routine *pwelch* with the parameter setting *window = hann(nfft), noverlap = 0* with *nfft = fs·T/n* (*n*: number of averages, here 10). The length of all measured time records is *T* = 10 s. Thus, we obtain a frequency resolution of $\Delta f = fs/nfft = n/T = 1$ Hz.

The spatial distribution of turbulence intensity and integral length given here are exclusively those due to fluctuations in axial (i.e. *z*-) direction (the co-ordinate system is depicted in Fig. 2). The axial velocity is divided up $c_z = \overline{c}_z + c_z'$ with the time mean value

$$\overline{c}_z = \frac{1}{T}\int\limits_{t_0}^{t_0+T} c\, dt\,. \tag{5}$$

Again the integration interval *T* is chosen 10 s. c_z' are the fluctuations with $\overline{c_z'} = 0$ by definition. The turbulence intensity is defined as

$$Tu = \frac{\sqrt{\overline{c_z'^2}}}{\overline{c}_z}\,, \tag{6}$$

with $\sqrt{\overline{c_z'^2}}$ being the rms-value of the axial velocity fluctuations. All velocities are taken at a certain location, hence *Tu* is the *local* turbulent intensity. The axial correlation length is determined assum-

ing the validity of Taylor's "frozen turbulence"-hypothesis (see e.g. in Hinze [16]) which allows setting $\dfrac{\partial}{\partial t} = -\overline{c}_z \dfrac{\partial}{\partial z}$. Integration of the auto-correlation function $R_{zz}(t) = \dfrac{\overline{c'_z(\tau)c'_z(\tau-t)}}{\overline{c'^2_z}}$ yields the integral time scale $I = \int_0^\infty R_{zz}(t)\,dt$. Here ∞ is replaced by t^* corresponding to the first zero-crossing of $R_{zz}(t)$. The time scale is multiplied by the local time mean velocity $\overline{c}_z$ to obtain the axial integral length scale

$$\Lambda_z = I\,\overline{c}_z. \tag{7}$$

It was found that the auto-correlation function and eventually the integral length scale depend on the length of the time record considered. Detailed investigations are given in [16]. In this work we subdivided the 10 s time record into 100 segments of 0.1 s and evaluate the auto-correlation function for each segment. An average of these 100 auto-correlation functions is used to determine the axial integral length scale.

In some acoustic models the turbulence statistics in the moving blade co-ordinate system are of more relevance. Because of the small stagger angle of the fan blades the length scale of a turbulent eddy in chord-wise direction of a blade corresponds more to the circumferential integral length scale in the stationary system than to the axial. This circumferential integral length scale was not measured here but in [17] by Schneider for a similar fan assembly.

For capturing the far field sound pressure and determining the sound pressure spectra the same parameters as for the velocity measurements apply. For all sound pressure levels, the reference pressure is $p_0 = 2 \cdot 10^{-5}$ Pa. All overall sound levels are the sum of narrow band levels from 100 to 10 kHz.

EXPERIMENTAL RESULTS

Tab. 2 gives an overview of the series of experiments reported in this presentation.

Turbulent inflow statistics. The upper two diagrams in Fig. 5 show integral turbulent inflow statistics across a diameter in the measuring plane. The overall flow rate is set to $\dot{V}_{design} = 0.65$ m^3/s and kept constant. Thanks to the HFC the turbulent intensity is less than 1 % at most locations outside of the wall boundary layer. The axial integral length scale varies between 5 and 30 mm which is in the order of the blade chord length (86 mm at the hub to 68 mm at the tip). The lower diagram presents the energy spectra (power spectral density) of the velocity fluctuations at different radial locations ($y = 84, 100, 118, 134, 142$ and 149 mm correspond to 20 %, 40 %, 60 %, 80 %, 90 % and 98 % relative blade height).

Table 2: Series of experiments

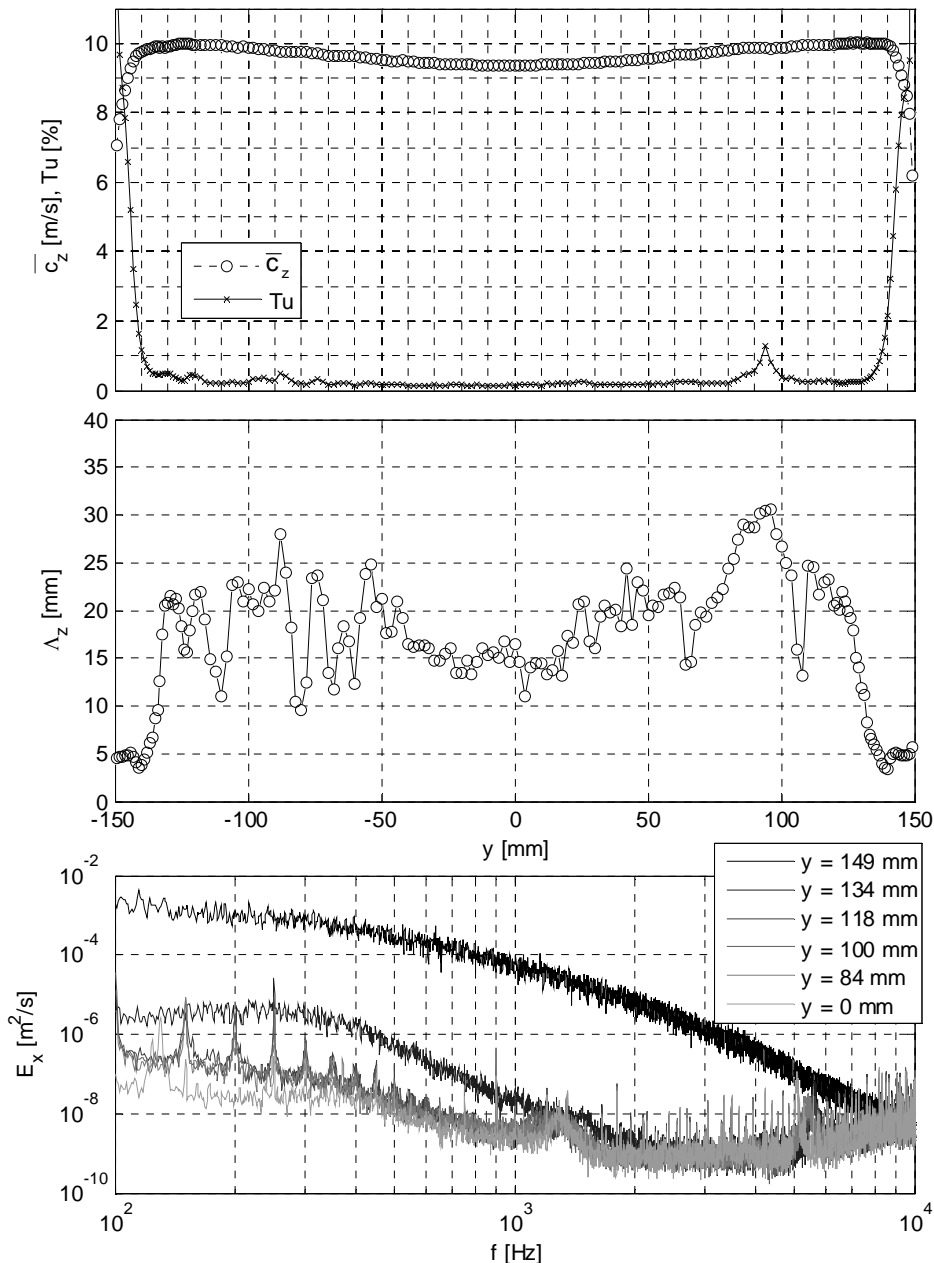| No.	Experiment	$s/d_2 = 0.1$ %	$s/d_2 = 1$ %	Operating point	Test rig
1	Turbulent inflow statistics	n.a.	n.a.	$\dot{V}_{design} = 0.65$ m^3/s	duct
2	Aerodynamic characteristics	x	x	(full range of $\dot{V}$)	chamber
3	Acoustic characteristics	x	x	(full range of $\dot{V}$)	duct
4	Acoustic spectra	x	x	$\dot{V}_{design} = 0.65$ m^3/s	duct

Figure 5: Upper: Axial mean flow velocity and local turbulence intensity, middle: Axial integral length scale; lower: energy spectra of velocity fluctuations (power spectral density) at different radial locations; $\dot{V}_{design} = 0.65\ m^3/s$

Overall characteristics. Fig. 6 presents the overall aerodynamic and acoustic performance characteristics. The effect of the tip gap is remarkable: Not only pressure rise and efficiency are degraded by the larger gap, but both, up- and downstream sound power level, are increased. The L_{W4}-characteristic differs slightly from the L_{W5}. An explanation for that is given in the next paragraph. Naively one would expect to see the maximum efficiency at the design flow rate. But one has to keep in mind that the total-to-*static* pressure rise and efficiency is plotted. The maximum of (the difficult to evaluate) total-to-*total* efficiency is always shifted to larger flow rates. For the small tip gap the stall point is well pronounced and indicated by the unsteadiness of the pressure rise and efficiency characteristic. It coincides well with the sudden increase of sound emitted. Both L_{W4} and L_{W5} stay nearly constant as the flow rate in increased. But because of the lack of an auxiliary fan the maximum flow rate within the acoustic tests is limited. On the other hand, the large tip gap is responsible for a smear of the stall point and a steady decrease of sound as the flow rate is increased.

Sound pressure and power spectra. The sound spectra at design flow rate are depicted in Fig. 7. Rows a) and c) represent the sound pressure spectra as measured by the duct and free field microphones, respectively. From those the sound power levels (rows b) and c)) are calculated. For a given tip gap size the sound power spectra in the free field and in the duct are similar but not identical (cp. e.g. b) left and d) left). One has to keep in mind that the fan radiates either upstream via the bell mouth inlet nozzle into the free field or downstream into the duct with its anechoic termination. The bell mouth inlet nozzle acts as an acoustically open termination and hence reflects the lower frequency components back to the duct.

The HFC provides a spatially rather homogeneous turbulent inflow to the rotor. This is reflected in the acoustic spectra since sound pressure levels at the blade passing frequency tones (multiples of z times n) are comparably low (note: a perfectly uniform inflow should result in broad band sound only). However, if one analyzed a series of short time non-averaged acoustic spectra one would detect a temporal variation of the levels at these tones of 2 - 3 dB, see Sturm and Carolus [18]. This can be of importance when comparing these experimental data with numerically predicted tones.
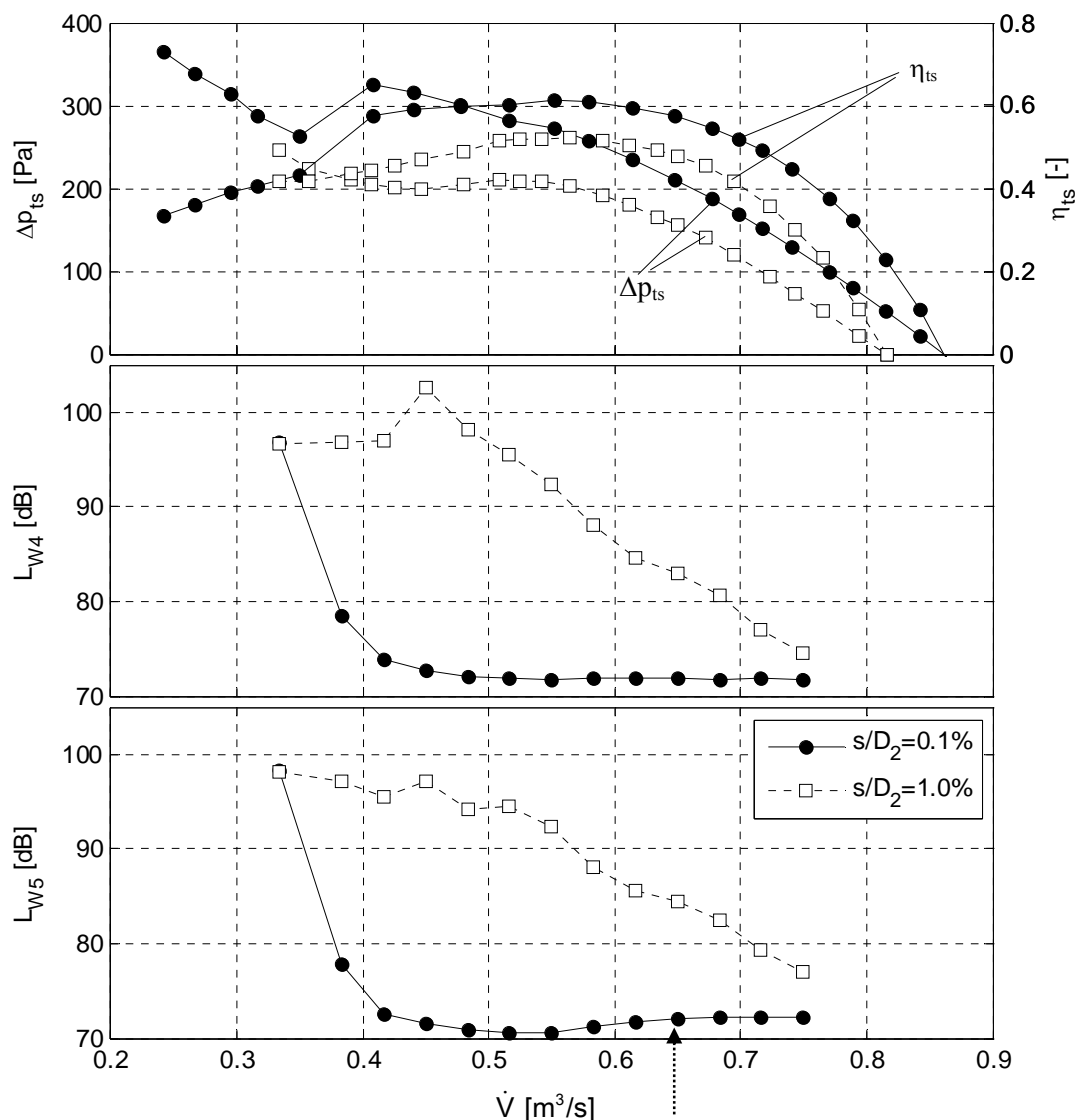

Figure 6: Overall performance and acoustic characteristics of USI7 for two different tip gaps; n = 3000 rpm, ρ = 1.16 kg/m³; dotted arrow indicates design flow rate

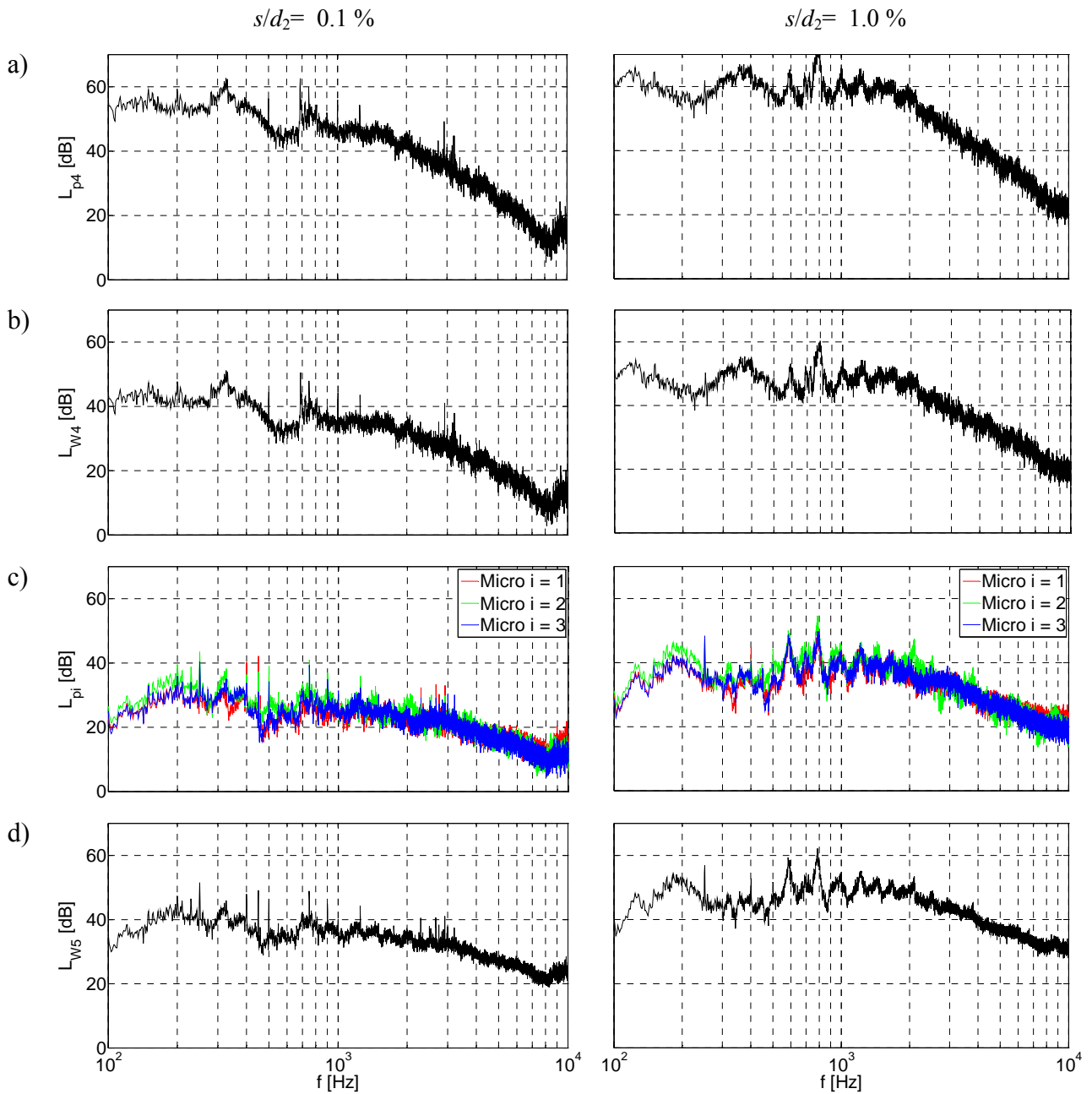$s/d_2 = 0.1\ \%$ $s/d_2 = 1.0\ \%$

Figure 7: a) Sound pressure level at downstream duct microphone, b) downstream (exhaust) sound power level L_{W4}, c) sound pressure level at the three upstream free field microphones, d) upstream (inlet) sound power level L_{W5}; $\dot{V}_{design} = 0.65\ m^3/s$, n = 3000 rpm, $\rho = 1.16\ kg/m^3$

UNCERTAINTIES

The measurement uncertainties procedures are described in detail in [19 - 21]. They are mainly based on the "Guide to the expression of uncertainty in measurement (GUM)" [22]. Estimates of uncertainties are stated in Tab. 3 in terms of the standard (relative) or absolute uncertainty ε_r and ε.

Table 3: List of uncertainties

static pressure	p	$\varepsilon_r \leq 0.5\ \%$
total-to-static efficiency	η_{ts}	$\varepsilon_r \leq 2\ \%$

volume flow rate	$\dot{V}$	$\varepsilon_r \leq 1\,\%$	
flow velocity	c_z	$\varepsilon_r \leq 1.5\,\%$	
overall duct sound power level	L_{W4}	$\varepsilon \leq 2$ dB	precision class 2 acc. to [13]
free field sound power level	L_{W5}	$\varepsilon \leq 2$ dB	precision class 1 acc. to [14], but less microphones used
narrow band sound pressure level	$L_p(f)$	$\varepsilon \leq 1$ dB	

CONCLUSIONS

In this paper a generic low pressure axial (rotor-only) fan and its experimentally determined aerodynamic and aero-acoustic performance characteristics are presented. In addition, the test facilities and test conditions for all aerodynamic and aero-acoustic performance are described in detail. The idea is to foster benchmarking of present and new steady-state and unsteady aerodynamic and eventually aero-acoustic prediction methods within the fan and turbomachinery community. Thus we will provide the full geometry of the fan as well as all experimental data to any individual[1].

NOMENCLATURE

a	m/s	speed of sound
A	m^2	area
C	m	chord length blade element
c_z	m/s	axial flow velocity in stationary frame of reference
d_1, d_2	m	hub -, nominal duct diameter
L_{p4}, L_{p5}	dB	downstream (exhaust), upstream (inlet) sound pressure level
L_{pi}	dB	free field sound pressure level at position i
L_{W4}, L_{W5}	dB	downstream (exhaust), upstream (inlet) sound power level
Ma	-	circumferential Mach number
n	rpm	rotor speed
Re	-	blade element Reynolds number
s	m	tip gap
Tu	%	local turbulent intensity
$\dot{V}$	m^3/s	volume flow rate
Δp_{ts}	Pa	total-to-static pressure rise
η_{ts}	-	total-to-static efficiency
Λ_z	m	axial integral length scale
ν	m^2/s	kinematic viscosity of air
ρ	kg/m^3	density of air

---

[1] Inquieries should be addressed to Thomas Carolus at the Institute of Fluid- and Thermodynamics, University of Siegen, Germany (thomas.carolus@uni-siegen.de) - we will provide a package of data free of charge.

BIBLIOGRAPHY

[1] Sturm, M., Carolus, T. – *Tonal Fan Noise of an Isolated Axial Fan Rotor due to Inhomogeneous Coherent Structures at the Intake.* Noise Control Engr. J. 60 (6), November-December **2012**, pp. 699-706

[2] Zhu, T., Carolus, T. – *Experimental and Numerical Investigation of the Tip Clearance Noise of an Axial Fan.* Proc. of the ASME, GT2013-94100, **2013**

[3] Sturm, M., Carolus, T. – *Large-Scale Inflow Distortions as a Source Mechanism for Discrete Frequency sound from Isolated Axial Fans.* 19th AIAA/CEAS Aeroacoustics Conference, **2013**

[4] Zhu, T., Carolus, T. – *Experimental and Unsteady Numerical Investigation of the Tip Clearance Noise of an Axial Fan.* Proc. of the ASME, TBTS2013-2034, **2013**

[5] Sturm, M., Carolus, T. – *Impact of the Large-Scale Environment on the Tonal Noise of Axial Fans.* Proc. IMechE Part A, J. Power and Energy 227(6) 703-710, **2013**

[6] Zhu, T., Carolus, T. – *Experimental and Numerical Investigation of Tip Clearance Noise of an Axial Fan Using a Lattice Boltzmann Method.* 21st International Congress on Sound and Vibration (ICSV 21), Bejing, **2014**

[7] Drela, M.: XFOIL – *An Analysis and Design System for Low Reynolds Number Airfoils, Conference on Low Reynolds Number Airfoil Aerodynamics.* University of Notre Dame, June **1989**.

[8] Carolus, T., Starzmann, R. – *An Aerodynamic Design Methodology for Low Pressure Axial Fans with Integrated Airfoil Polar Prediction.* Proc. of the ASME, GT2011-45243, **2011**

[9] Scheimann, J., Brooks, J. D. – *A Comparison of Experimental and Theoretical Turbulence Reduction from Screens, Honeycomb and Honeycomb-Screen Combinations.* 11th Aerodynamic Testing Conference, Colorado Springs, USA, AIAA Technical Papers, pp. 129-137, **1980**

[10] SAE International – *Methods of Controlling Distortion of Inlet Airflow During Static Acoustical Tests of Turbofan Engines and Fan Rigs.* Aerospace Information Report, **1985**

[11] Groth, J., Johansson, A. V. – *Turbulence Reduction by Screens.* J. of Fluid Mechanics, Vol. 197, pp. 139-155, **1988**

[12] DIN 24163 – *Ventilatoren, Teil 2: Leistungsmessung - Normprüfstände (Fans, part 2: performance tests - standardized test rigs)*, **1985**

[13] DIN ISO 5136 – *Bestimmung der von Ventilatoren und anderen Strömungsmaschinen in Kanäle abgestrahlten Schallleistung*, **2000**

[14] ISO 13347-3 – *Industrial fans - Determination of fan sound power levels under standardized laboratory conditions, Part 3: Enveloping surface methods.* International Standard **2004**-08-14 with technical corrigendum **2006**-11-15

[15] Zhu, T., Carolus, T. – *Akustische Nachrechnung von Ventilatoren.* Final report F60 001 B of the Universität Siegen, Institut für Fluid- und Thermodynamik, Fachgebiet Strömungsmaschinen to the Forschungsvereinigung für Luft- und Trocknungstechnik e. V. (FLT), Frankfurt/M, Project No. AiF 16773 N/2, **2012**

[16] Hinze, J.O. – *Turbulence.* 2nd edition, McGraw-Hill, **1975**

[17] Carolus, T., Schneider, M., Reese, H. – *Axial flow fan broad-band noise and prediction.* J. of Sound and Vibration 300 (**2007**) pp. 50-70

[18] Sturm, M., Carolus, T. – *Unsteadiness of Blade-Passing Frequency Tones of Axial Fans.* 21st International Congress on Sound and Vibration (ICSV 21), Bejing, **2014**

[19] Hensel, K. – *Konzeption eines Ventilatorprüfstandes nach DIN 24163*, Final thesis No. A93030003 at the University of Siegen, **1993**

[20] Winkler, J. – *Investigation of Trailing-Edge-Blowing on Airfoils for Turbomachinery Broadband Noise Reduction.* Ph.D. Dissertation University of Siegen, Germany, Shaker Verlag Aachen, **2011**

[21] DIN V EN V 13005 – *Leitfaden zur Angabe der Unsicherheit beim Messen*, **1999**

[22] ISO – *Uncertainty of Measurement - Part 3: Guide to the Expression of Uncertainty in Measurement* (GUM:1995), **2008**